*Supplementary information*

# Tyrosinase-catalyzed phenol-mediated immobilization of β-agarase on L-lysine-coated magnetic particles for the production of neoagarooligosaccharides from *Gelidium amansii*

Teklebrahan G. Weldemhret[†,§], Grace M. Nisola[†,§], Kristine Rose M. Ramos[†], Angelo B. Bañares[†], Kris Niño G. Valdehuesa[†,*], Won-Keun Lee[‡,*], Wook-Jin Chung[†,*]

[†] Department of Energy Science and Technology (DEST), Energy and Environment Fusion Technology Center ($E^2$FTC), Myongji University, Myongji-ro 116, Cheoin-gu, Yongin City 17058, Gyeonggi Province, South Korea

[‡] Division of Bioscience and Bioinformatics, Myongji University, Myongji-ro 116, Cheoin-gu, Yongin City 17058, Gyeonggi Province, South Korea

[§] co-first authors

[*]*Corresponding authors: (W.-J. Chung) wjc0828@gmail.com; (W.-K. Lee) wklee@mju.ac.kr; (K.N. Valdehuesa) krisnino87@gmail.com*

*Tel.: (82)-31-330-6687; Fax: (82)-31-337-2902*

Number of pages: **31**
Number of Figures: **19**
Number of Tables: **5**

## TABLE OF CONTENTS

***Materials***

Iron(III) chloride hexahydrate (>99%, $FeCl_3 \cdot 6H_2O$) and dinitrosalicylic acid (98%, DNS) were purchased from Acros Organics (NJ, USA). Ammonium hydroxide solution (25~30 wt. % $NH_3$ in water, $NH_4.OH$), ammonium sulfate (>99%, AS) and hydrochloric acid (35% HCl) was procured from Daejung Chemicals and Metals Co. Ltd (South Korea). Tyrosinase from *Agaricus bisporus* (T3824, ≥1000 U $mg^{-1}$), lysozyme (≥40, 000 U $mg^{-1}$), L-Lysine monohydrochloride (≥98%, $H_2N(CH_2)_4CH(NH_2)CO_2H \cdot HCl$), Iron(II) chloride tetrahydrate (99%, $FeCl_2 \cdot 4H_2O$), isopropyl-β-D-thiogalactopyranoside (≥99%, IPTG), bovine serum albumin (≥96%, BSA), D-galactose (≥99%, D-Gal), glutaraldehyde (Grade II 25% in $H_2O$, GA) and glycine (≥99%) were purchased from Sigma Aldrich (USA). Kanamycin sulfate (Kan) was from Biosesang (South Kora) while Tris base (99.8%) was procured from Fisher Scientific (Belgium). Phenol (99%) was from Junsei Chemical Co., Ltd. (Japan) while sodium hydroxide (97%, NaOH) was procured from Kanto Chemical Co., Inc. (Tokyo, Japan). Glycerol (99%) was purchased from Samchun (South Korea). Potassium phosphate monobasic (>99%, $KH_2PO_4$), potassium phosphate dibasic (>99%, $K_2HPO_4$) and sodium citrate tribasic dehydrate (99%, $HOC(COONa)(CH_2COONa)_2 \cdot 2H_2O$) were procured from Duksan Pure Chemicals (Ansan, South Korea). Citric acid monohydrate (>99.5%, $HOC(COOH)(CH_2COOH)_2 \cdot H_2O$) was from Showa (Japan). Agarose (gelling temperature 1.5% w $v^{-1}$: 36 ±1.5 ºC) was from iNtRON Biotechnology, Inc (South Korea). Sugar standards for neoagarohexaose (≥99%, NA6) and neoagarotetraose (≥99%, NA4) were purchased from DyneBio (South Korea) and stored in a refrigerator at -20 ºC until use for confirmation analysis of hydrolysis products. The water utilized in this study was ultrapure deionized water (Milli-Q Millipore 18.2 M Ω.cm conductivity at 25 ºC).

***Construction of pET28a-aga2Y5N***

The plasmid pET28a-aga2Y5N is an expression vector for Aga2, which contains five Tyrosine residues (Y5N) without its native N-terminal signal peptide but has a 6×Histidine-tag at the N-terminal of the peptide sequence. Polymerase chain reaction (PCR) was performed using the following oligonucleotide pair (5'→3'): Forward – CTC GGA TCC TAT TAT TAT TAT TAT GAT AAT GAA TCT ACA GAT AA and Reverse – CTC GAA TTC ATC TGC TTT AAC CGG TTT AA. The PCR product was ligated into the *Bam*HI/*Eco*RI recognition sites of pET28a (Invitrogen, Korea), resulting in the expression vector pET28a-aga2Y5N. To verify the fidelity of the recombinant DNA, restriction mapping and DNA sequencing were performed.

***Expression and purification of β-agarase***

The *E. coli* expression strains for Aga2 and Aga2Y5N were cultured in LB broth and incubated at 37 °C until the optical density at 600 nm reached ~0.4 - 0.6 absorbance units. Protein expression was induced by adding 0.1 mM IPTG and the cultures were further incubated at 20 °C for 16 h. The broths were then centrifuged at 4 ºC, and the collected cells were re-suspended in ice cold LEW buffer (50 mM $NaH_2PO_4$, 300 mM NaCl, pH 8.0). Lysozyme was added to a final concentration of 1 mg $mL^{-1}$ and incubated at 4 °C for 30 min. The mixture was ultrasonicated (BRANSON, Digital sonifier, Branson 450) for 5 min (10% amplitude, 10 s bursts, 10 s cool down). Cell debris was separated by centrifugation at 13,000 rpm and 4 °C for 10 min. The target proteins were then purified from the supernatant using Protino® Ni-TED pre-packed column (Macherey-Nagel, BMS, Korea). Protein fractions were analyzed by sodium dodecyl sulfate polyacrylamide gel electrophoresis (SDS-PAGE) while sample concentrations were quantified through Bradford protein assay kit (Bio-Rad Laboratories, USA) using bovine serum albumin as standard.

***CLEA preparation by glutaraldehyde cross-linking as control sample***

The CLEA of Aga2 using GA was prepared according to the method described elsewhere.[1] GA (20% w $v^{-1}$) was added into Aga2 (0.5 mg $mL^{-1}$) solution in potassium phosphate buffer (50 mM, pH 7.0) in the absence (Aga2-GA) or presence of 80% saturated AS solution (Aga2-GA + AS) under gentle stirring at 4 °C for 16 h. Then the suspensions were centrifuged at 13 000 rpm for 10 min at 4 °C then washed three times with 50 mM Tris-Cl buffer (pH 7.0) and finally stored in 50 mM Tris-Cl (pH 7.0) at 4 °C.

***Preparation of Lys@$Fe_3O_4$ particles***

Lys@$Fe_3O_4$ particles were prepared *in-situ* via one-pot synthesis (Scheme 1, main text). Precursors $FeCl_3{\cdot}6H_2O$ (1.1 g) and $FeCl_2{\cdot}4H_2O$ (0.4 g) were dissolved in 150 mL DI water at 2:1 molar ratio and agitated vigorously (12,000 rpm) under $N_2$ atmosphere at 60 °C for 15 min. Thereafter, L-lysine monohydrochloride (3.2 g) was rapidly added and the mixture was stirred for another 20 min. $NH_4OH$ solution (25~30 wt% $NH_3/H_2O$) was added dropwise (~ 20 mL) while being mixed vigorously under $N_2$ atmosphere. The solution was left to stand for 6 h at 60 °C before magnetically collecting the final product Lys@$Fe_3O_4$ NPs, which was subsequently washed four times with DI water and vacuum dried overnight at 50 °C. Bare $Fe_3O_4$ NPs were synthesized similarly but without L-lysine addition.

***Characterization of magnetic CLEAs***

The textural property of bare $Fe_3O_4$ and Ly@$Fe_3O_4$ was observed through powder X-ray diffraction (XRD) in a Bruker AXS D8 focus X-ray diffractometer (Cu-Kα radiation, step size 0.03° at 4° $min^{-1}$ scan speed) from 20° to 80°. The morphology of the samples was examined using field emission scanning electron microscope (FE-SEM FEI XL-30 FEG Hitachi SU-70, Japan) operated at 15.0 kV. Transmission electron microscope (TEM) images were recorded using the FEI Talos F200 X (Thermo Fisher, USA) at 120 kV - 200 kV with a 2k × 2k CCD camera (Gatan, US1000). Fourier transform infrared (FTIR) spectroscopy was carried out using a NICOLETiS5 FT-IR spectrophotometer (Thermo Scientific) through standard KBr disc method within 400 - 4000 $cm^{-1}$ at room temperature. Thermal decomposition behavior was examined using a Thermo-Gravimetric Analyzer (Mettler Toledo, DSC 823e) from room temperature to 800 °C at 10 °C $min^{-1}$ heating rate under $N_2$ (50 mL $min^{-1}$). Dynamic light scattering (DLS) measurements were performed on a Zetasizer Nano ZS (Malvern, South Korea). Hydrodynamic diameter was measured at a back-scattering angle of 173° with a He/Ne laser (λ = 633 nm) at 25 °C. Reported values are averages of at least triplicate measurements. Their magnetic property was measured using a vibrating sample magnetometer (MPMS3-Evercool (SQUID VSM), Quantum Design Inc.).

***Enzyme assays via DNS method***

Agarase activity assay was performed using the dinitrosalicylic acid (DNS) method. Free enzymes, free CLEA and magnetic CLEA were incubated with 0.2 % (w $v^{-1}$) agar in 50 mM Tris-Cl (pH 8.0) for 5 min at 45 °C. The mixture was added with 1 volume of DNS reagent (6.5 g DNS, 325 mL 2 M NaOH, and 45 mL glycerol in 1 L deionized water) and placed in boiling water for 10 min. After cooling to room temperature, the absorbance was measured at λ = 540 nm. Total reducing sugars (TRS) produced during hydrolysis were quantified using D-galactose as the standard compound. The optimum pH (3 – 10) and temperature (25 – 75 °C) for the activity of CLEA and magnetic CLEA were determined using different buffers depending on the pH requirement: (i) 50 mM citrate buffer for pH 3 – 6, (ii) 50 mM Tris-Cl buffer for pH 7 – 8, and (iii) 50 mM glycine-NaOH buffer for pH 9 –10.

***Enzyme loading determination on magnetic CLEAs***

The amount of enzymes immobilized on Lys@$Fe_3O_4$ was determined from the difference between its concentrations in the supernatant before ($P_o$) and after ($P_i$) magnetic CLEA preparation. Since the tyrosinase is also present in the supernatant, methods such as Bradford or Lowery assay cannot be used to determine $P_i$. Thus, standard agarase activity ($A$) curves were constructed from 0.01- 0.4 mg $mL^{-1}$ of Aga2 or Aga2Y5N.[2] After immobilization, $A$ values were measured in the supernatant then were used to the obtain $P_i$ values through the linear equations presented in **Fig. S1**.

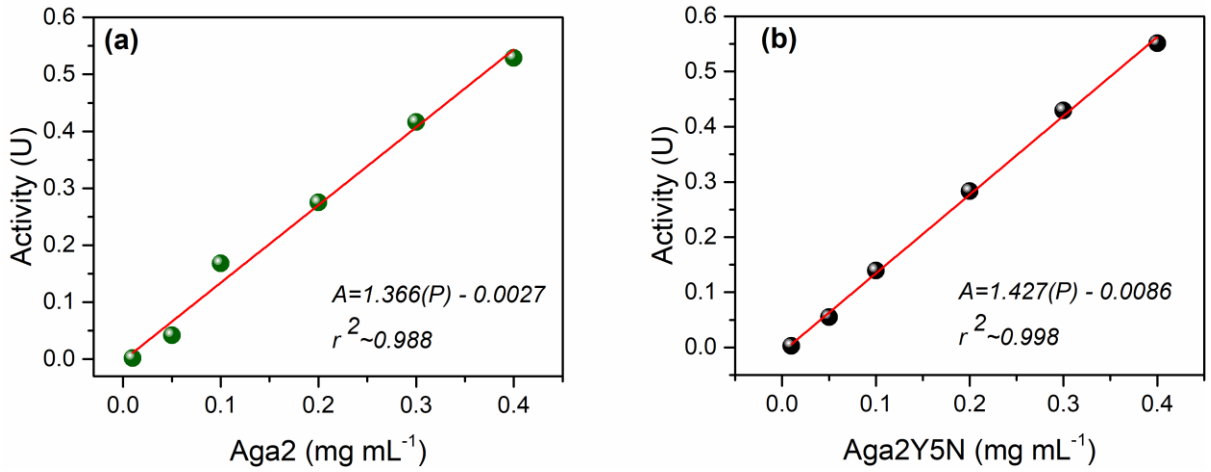


**Fig. S1** Standard curves of agarase activity against protein concentration: (a) Aga2 and (b) Aga2Y5N.

With known $P_o$ and $P_i$ values, enzyme loadings (as mg $g^{-1}$ Lys@$Fe_3O_4$) were determined using Eq. S1, where $m$ (as g) is the mass of Lys@$Fe_3O_4$ used during immobilization and $V$ is the volume of protein solution (as mL).

$$\frac{(P_o - P_i)}{m} \times V \qquad \text{(S1)}$$

***Kinetics of magnetic CLEAs***

The kinetic parameters of Aga2, Aga2Y5N and Aga2Y5N-TP@Lys@$Fe_3O_4$ were determined by monitoring the increase in the total reducing sugar (TRS) at known time and varying agarose concentrations: 0.05 to 0.8 mg $mL^{-1}$ in 50 mM Tris-Cl, pH 7.0). Briefly, 1.2 mg protein in each biocatalyst was incubated with agarose at 45 °C for both Aga2 and Aga2Y5N, and at 55 °C for Aga2Y5N-TP@Lys@$Fe_3O_4$. Samples were withdrawn at various hydrolysis times (2.5, 5.0, 7.5 and 10 min) for TRS quantification using DNS method. The slope of the time profile was derived as the initial reaction rate ($v_o$), which is the rate of TRS production (μM $min^{-1}$) by the bio-catalyst. With known $v_o$ at various agarose concentrations [S] (g $L^{-1}$), $K_m$ and $V_{max}$ were estimated by performing nonlinear fitting with the Michaelis−Menten kinetic model (Eq. S2) where $V_{max}$ (μM $min^{-1}$) is the maximum agarose hydrolysis rate and $K_m$ (g $L^{-1}$) is the Michaelis−Menten constant pertaining to [S] at half of $V_{max}$. Catalytic turnover number, $k_{cat}$ ($s^{-1}$) was calculated by dividing $V_{max}$ with the total amount of enzyme used. OriginPro 2016 was used for curve fitting.

$$v_o = \frac{V_{max}[S]}{K_m + [S]} \quad \text{(S2)}$$

***Sol-gel transition temperature determination of agar***

The sol–gel transition temperature of the extracted agar was monitored by measuring the viscosity of 3.4% (w $v^{-1}$) agar solution in 50mM Tris-HCl (pH 7.0) while being cooled from 75 $^{o}$C to 5 $^{o}$C in a circulating water bath. The sudden increase in viscosity of the agar solution is recorded as the sol-gel temperature of the sample.

***Thin-layer chromatography (TLC) analysis of hydrolysis products***

TLC was performed on the hydrolysis products of Aga2Y5N in duplicates on silica plate, which was then developed using n-butanol-ethanol-water (3:1:1, v/v/v) solvent. The reaction products were visualized using 10% (v $v^{-1}$) $H_2SO_4$ and 0.2% (w $v^{-1}$) resorcinol in ethanol followed by heat exposure. The hydrolysis products NA4 and NA6 were identified based on the TLC bands of known samples as sugar standards purchased from Biodyne (Korea).

***High-Performance Liquid Chromatography (HPLC) analysis of hydrolysis products***

The hydrolysates of Aga2Y5N-TP@Lys@$Fe_3O_4$ were analyzed by HPLC (Waters 2414 HPLC) equipped with a Refractive Index Detector (RID) and a BioRad Aminex HPX- 87H Ion Exclusion column (300 mm × 7.8 mm). Analysis was performed at column temperature of 55 $^{o}$C using 40% (v $v^{-1}$) acetonitrile in 5 mM trifluoroacetic acid as mobile phase which was delivered at 0.4 mL $min^{-1}$. Comparison with sugar standards NA4 and NA6 solutions purchased from Biodyne (Korea) was done to confirm the identity of the products.

***NMR analysis hydrolysis products***

The hydrolysis products of Aga2Y5N-TP@Lys@$Fe_3O_4$ were examined using $^{13}$C NMR, from reactions carried out in DI water. The soluble products were separated from the magnetic biocatalyst and unreacted agarose through magnetization and centrifugation (13,000 rpm) at 4 $^{o}$C for 20 min. The samples were run on TLC plates and the spots which match with those of NA4 and NA6 sugar standards were scraped with a razor then placed in separate tubes without sulfuric acid treatment. The products were dissolved in 100% ethanol to precipitate impurities and centrifuged (13,000 rpm) at 4 $^{o}$C for 20 min to remove the insoluble silica particles and impurities. Ethanol was removed by evaporating *in vacuo* (BUCHI Pervaporator R-200) at 45 $^{o}$C. The dried powder was dissolved in $D_2O$ and the spectra were recorded using Fourier transform nuclear magnetic resonance spectroscopy (FT-NMR) (Varian, 400-MR). MestReNova software was used to process the $^{13}$C-NMR results.

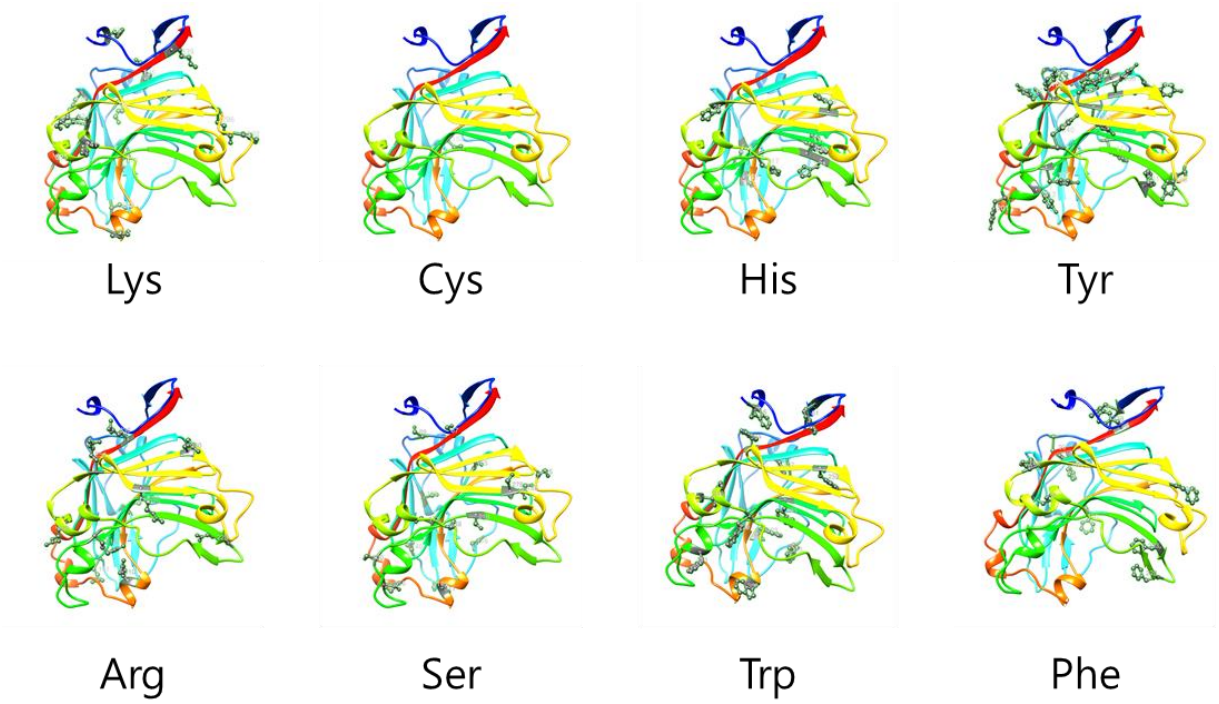


**Fig. S2** 3D tertiary structure prediction of Aga2 showing each of the amino acid (AA) residues that could potentially react with glutaraldehyde (GA) and/or tyrosinase. The 3D structure was generated using the *Protein Homology/analogY Recognition Engine* V2.0 web portal.[3] The resulting 3D model for Aga2 has 100% confidence with a coverage of 75% using the template PDB no. c104zA assigned to the 3D structure of ß-agarase from *Zobellia galactanivorans*. Blue to Red – N- to C-terminal.

From literature, it is known that for enzyme cross-linking, Lys, Cys, His, Tyr, Arg, Ser, Trp, Phe residues could react with GA[4,5] whereas Lys, Cys and Tyr can be activated by tyrosinase[6,7,8] in the presence of phenolic molecules, either added as external reagent or from Tyr residues. The 3D structures of Aga2 above reveal the number of reactive AAs for GA and/or tyrosinase. The total = buried AA + exposed AA were tabulated in Table S1 (next page) to roughly estimate the reactive sites available for each type of cross-linker.

**Table S1.** Number of reactive AAs in Aga2 that could participate in GA or tyrosinase cross-linking. Symbol (•) indicates reactivity. Only the exposed AAs were finally counted as estimates for the reactive sites.

| Amino acids | Number of residues | | GA | T only or T+P |
|---|---|---|---|---|
| | Exposed | Buried | | |
| Lysine | 14 | 3 | • | • |
| Cysteine | 0 | 1 | • | • |
| Histidine | 6 | 8 | • | |
| Tyrosine | 7 | 8 | • | • |
| Arginine | 6 | 4 | • | |
| Serine | 8 | 9 | • | |
| Tryptophan | 2 | 10 | • | |
| Phenylalanine | 2 | 7 | • | |
| Approximate number of reactive sites for cross-linking (exposed AA only): | | | **45 exposed AA** | **21 exposed AA** |

Given the number of exposed AAs, **Table S1** reveals that there are around **45 AAs** with reactive sites available for GA random cross-linking whereas there are only **21 AAs** for tyrosinase. From these estimates, tyrosinase is a *relatively* more selective route than GA for Aga2 cross-linking hence was selected for the CLEA preparation in this study. Moreover, the extent of enzyme cross-linking with phenol addition can be more easily controlled than GA, as the latter is more reactive and random, which could also involve many AAs that are critical to substrate binding.

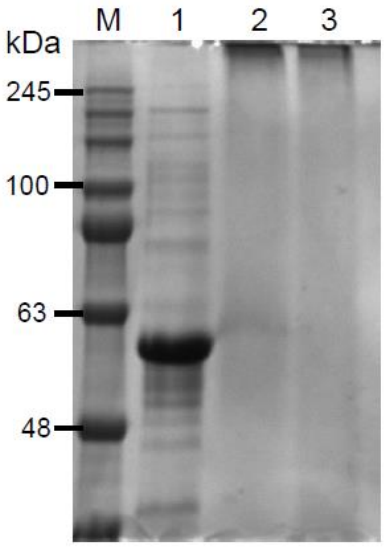


| CLEA | Recovered activity (%) |
|---|---|
| Aga2-GA | 4.9 ± 0.65 |
| Aga2-GA + AS | 13.3 ± 1.60 |

**Fig. S3** SDS page of free Aga2 (Lane 1) and its CLEA prepared by glutaraldehyde (GA) crosslinking (Lane 2: Aga2-GA) and GA-crosslinking with ammonium sulfate (AS) precipitation (Lane 3: Aga2-GA+AS). Lane M : standard MW marker**.**

The clean SDS lanes for Aga2-GA (**2**) and Aga2-GA+AS (**3**) indicates successful CLEA flocs formation as they cannot migrate through the gel. However, it was noticeable that most of the Aga2-GA CLEA were not stable in the buffer as they eventually solubilized, thus its low % recovered activity (< 5%). Meanwhile, the stability of Aga2-GA+AS CLEA was slightly improved, thus, its slightly higher % recovered activity (~ 13%). However, this value is still very low. The low % recovered activities strongly suggest unstable CLEA formation and possible participation of critical sites for substrate binding or catalytic activity during GA-mediated cross-linking. This motivated the use of other cross-linking methods such as tyrosinase-catalyzed cross-linking with or without phenol mediation.

The use of the proposed cross-linking technique (i.e. tyrosinase-catalyzed Aga2 or Aga2Y5N CLEAs with phenol mediation) was later proved to be sufficient and effective as almost all of the prepared free CLEAs have better % recovered activities (Table 1, main article) than the control GA-cross-linked CLEAs.

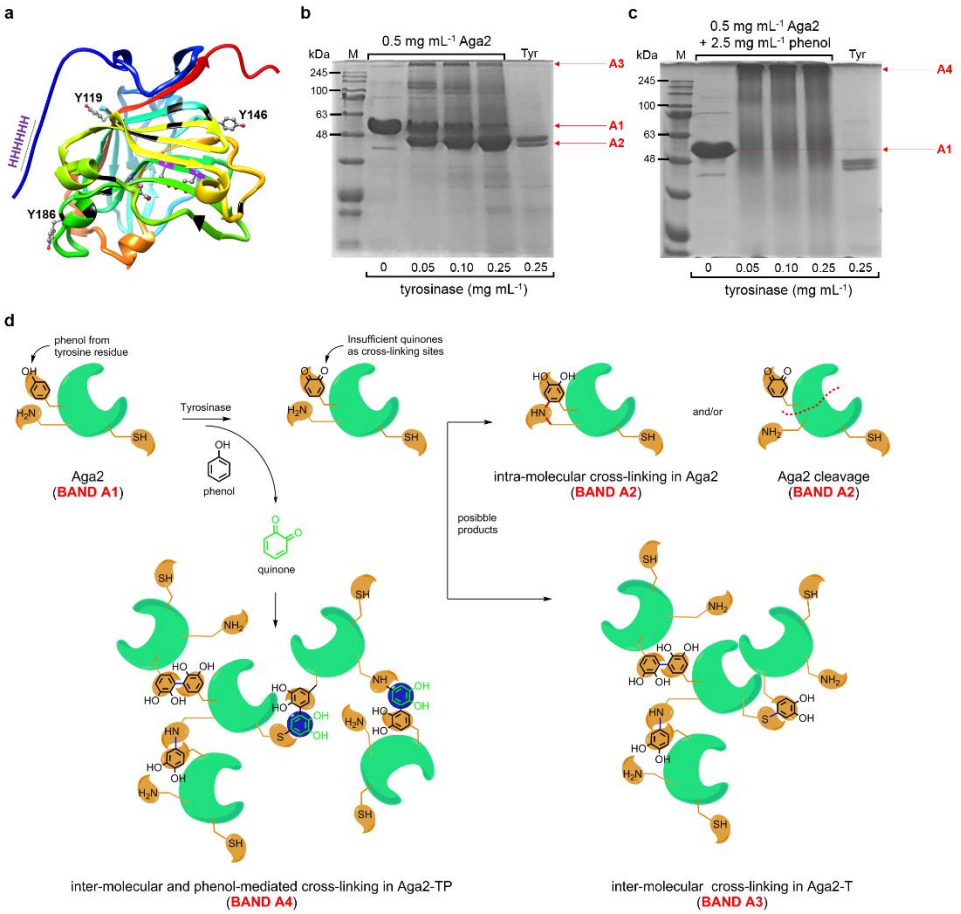


**Fig. S4** 3D tertiary structure prediction (a) and protein gels of Aga2 in the presence of tyrosinase (Aga2-T system, b) and tyrosinase with phenol addition (Aga2-TP,c). Proposed reactions involved during cross-linking and possible products for each system are matched with the SDS page labels (d). The apparent size of Aga2 is ~58 kDa. The 3D structure was generated using the *Protein Homology/analogY Recognition Engine* V2.0 web portal.[3] The resulting 3D model for Aga2 has 100% confidence with a coverage of 75% using the template PDB no. c104zA assigned to the 3D structure of ß-agarase from *Zobellia galactanivorans*. Blue to Red – N- to C-terminal. Polypeptide tags are designated at the N-terminal. Surface-exposed tyrosine residues (Y) are shown (number represent the position of the amino acid residue based on the native protein sequence of Aga2: GenBank ID. ATI14840.1). Black parts of the 3D structure represent tyrosine residues located within the protein.

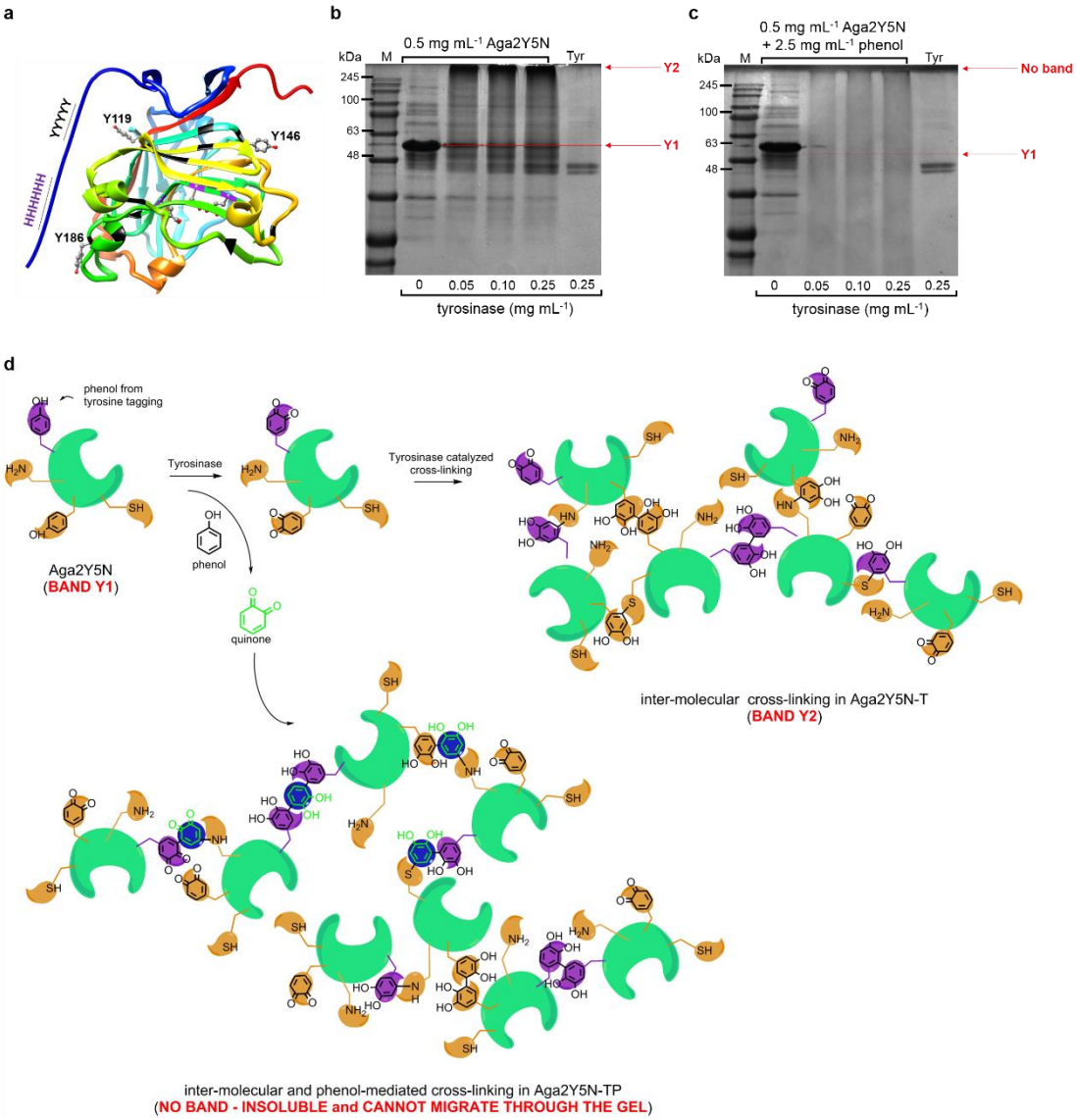


**Fig. S5** 3D tertiary structure prediction (a) and protein gels of Aga2Y5N in the presence of tyrosinase (Aga2Y5N-T system, b) and tyrosinase with phenol addition (Aga2Y5N-TP,c). Proposed reactions involved during cross-linking and possible products for each system are matched with the SDS page labels (d). The apparent size of Aga2Y5N is ~58 kDa. The 3D structure was generated using the *Protein Homology/analogY Recognition Engine* V2.0 web portal.[3] The resulting 3D model for Aga2 has 100% confidence with a coverage of 75% using the template PDB no. c104zA assigned to the 3D structure of ß-agarase from *Zobellia galactanivorans*. Blue to Red – N- to C-terminal. Polypeptide tags are designated at the N-terminal. Surface-exposed tyrosine residues (Y) are shown (number represent the position of the amino acid residue based on the native protein sequence of Aga2: GenBank ID. ATI14840.1). Black parts of the 3D structure represent tyrosine residues located within the protein.

**Table S2.** Enzyme loading in magnetic CLEAs.

| Type | Aga2 (mg $g^{-1}$ Lys@$Fe_3O_4$) | Aga2Y5N (mg $g^{-1}$ Lys@$Fe_3O_4$) |
|---|---|---|
| **-@Lys@$Fe_3O_4$** | 4.1 ± 32 | 2.8 ± 16 |
| **-T@Lys@$Fe_3O_4$** | 3.0 ± 25 | 10.3 ± 0.1 |
| **-TP@Lys@$Fe_3O_4$** | 22.5 ± 21 | 26.1 ± 1.8 |

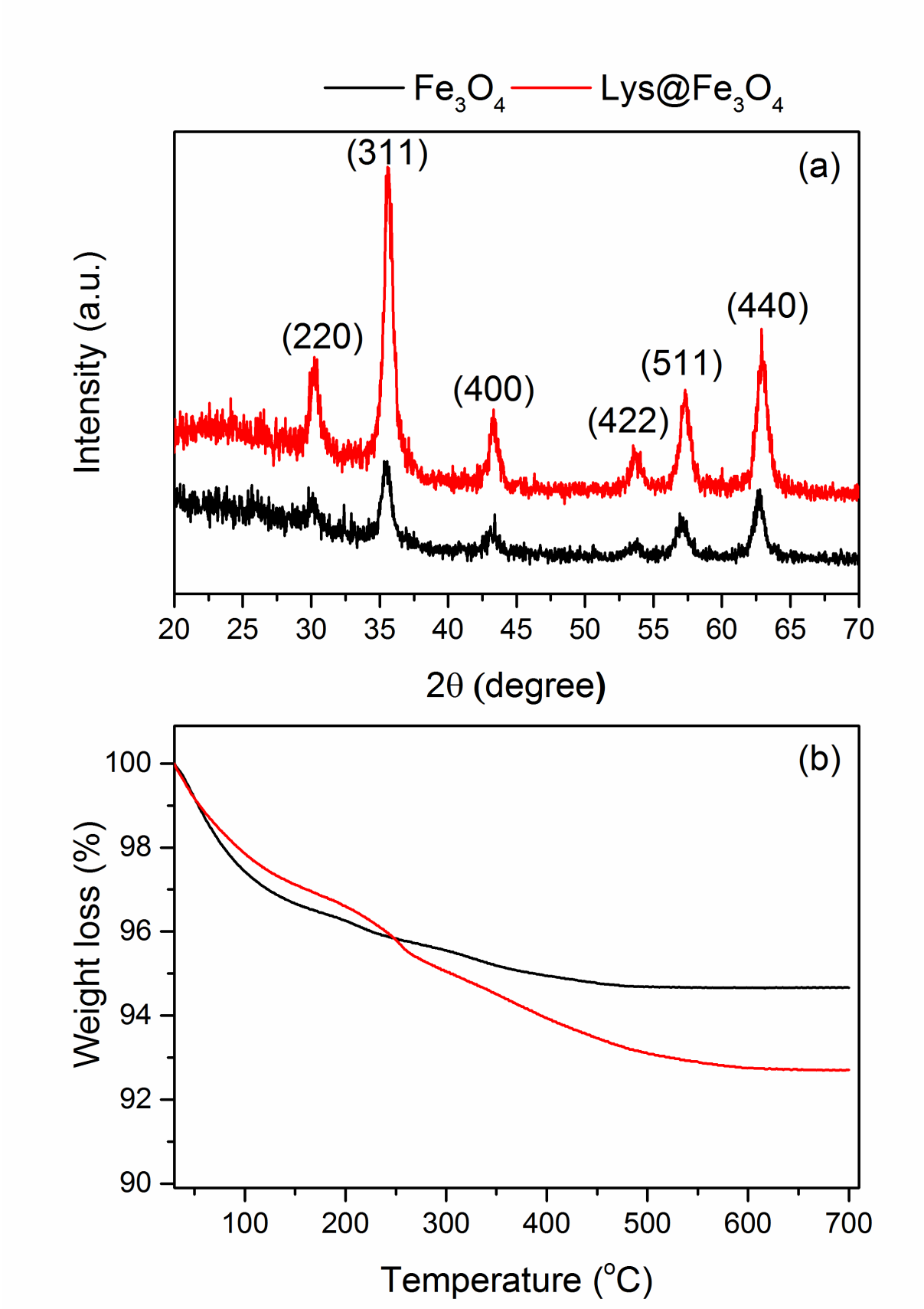


**Fig. S6 (a)** XRD diffraction patterns and (b) TGA curves of $Fe_3O_4$ and Lys@$Fe_3O_4$.

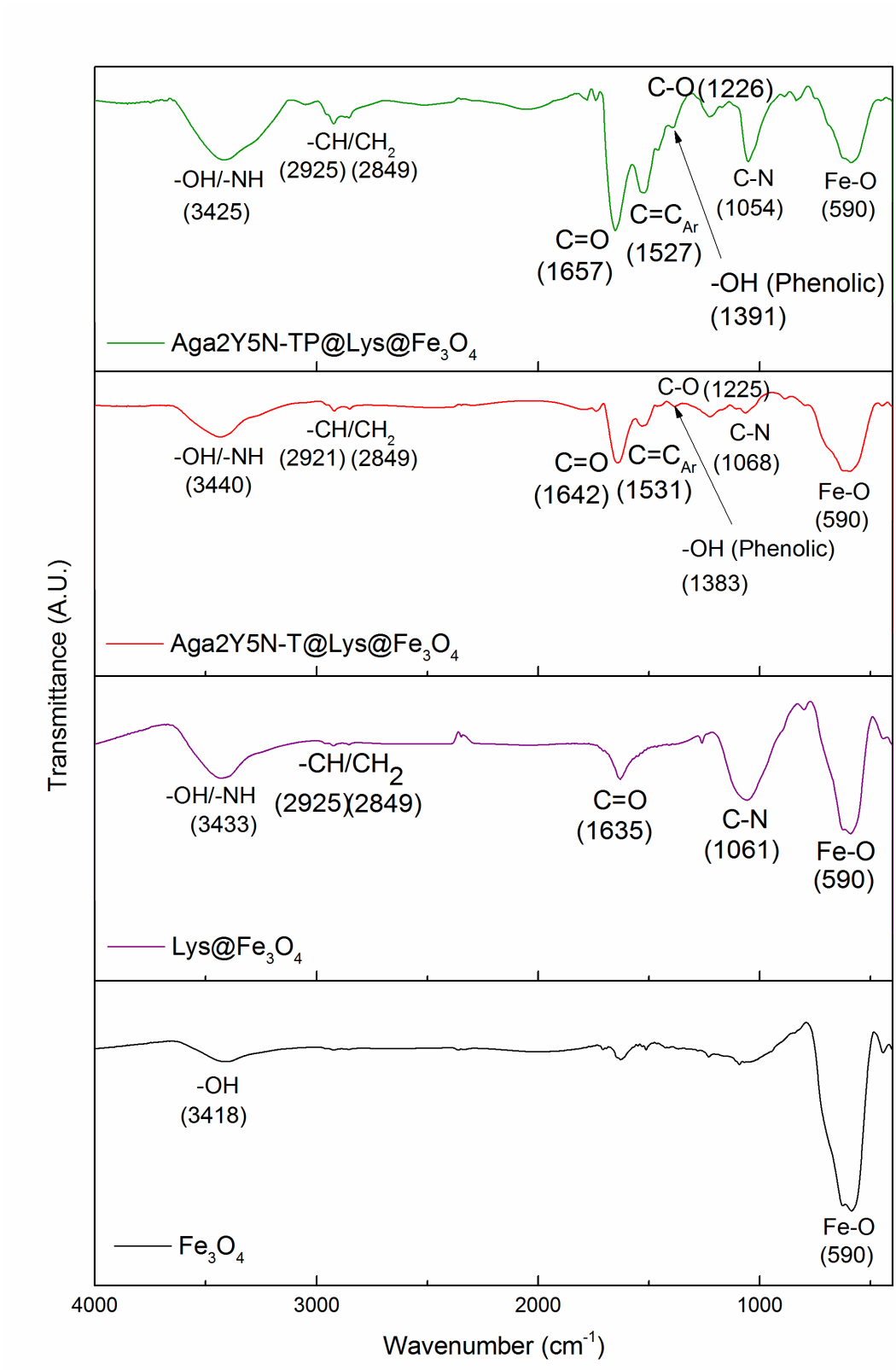


**Fig. S7** FT-IR spectra of magnetic supports and magnetic CLEA of Aga2Y5N.

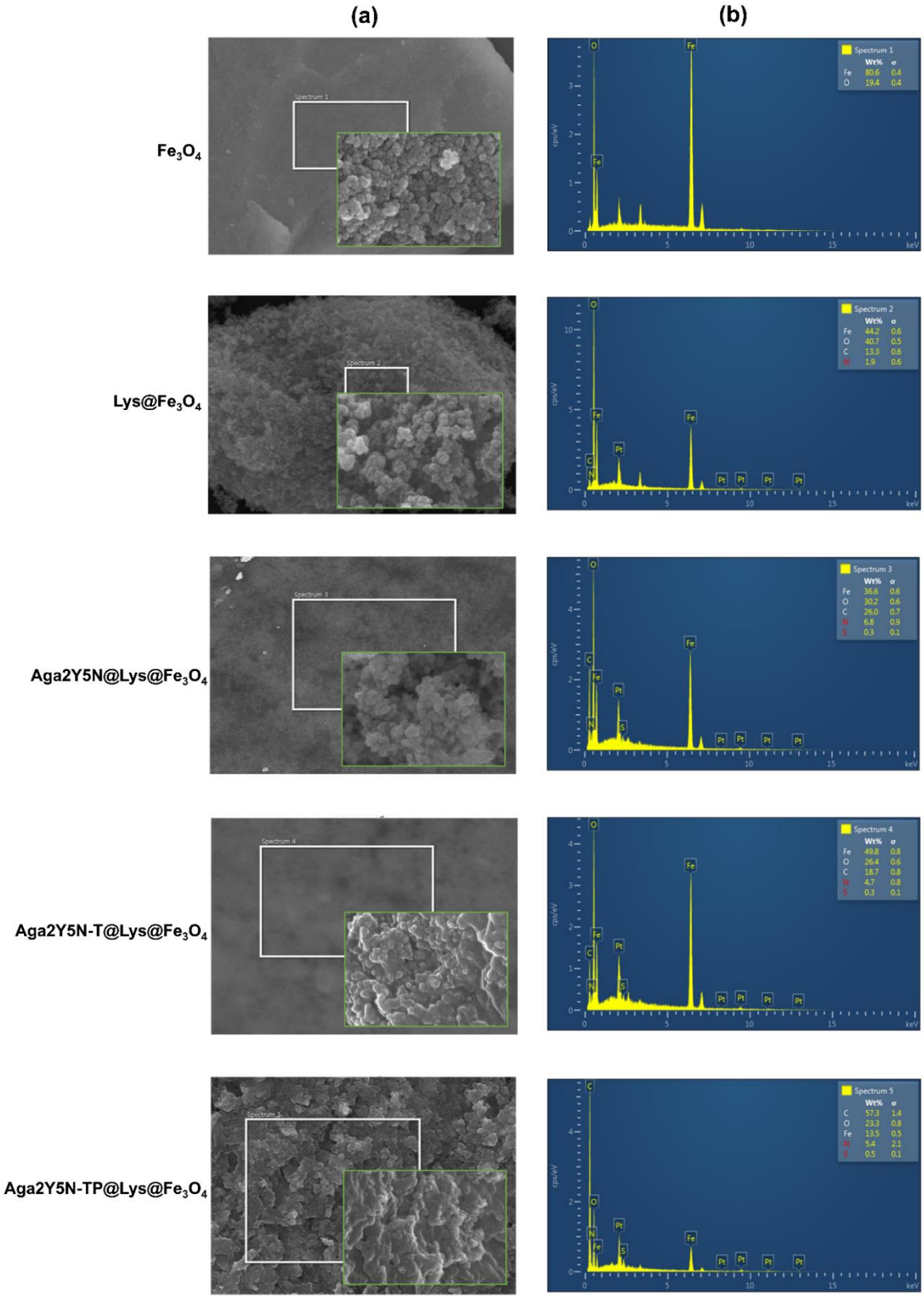


**Fig. S8** (a) SEM images (inset at higher magnification) and (b) EDX analysis of magnetic supports and magnetic CLEA.

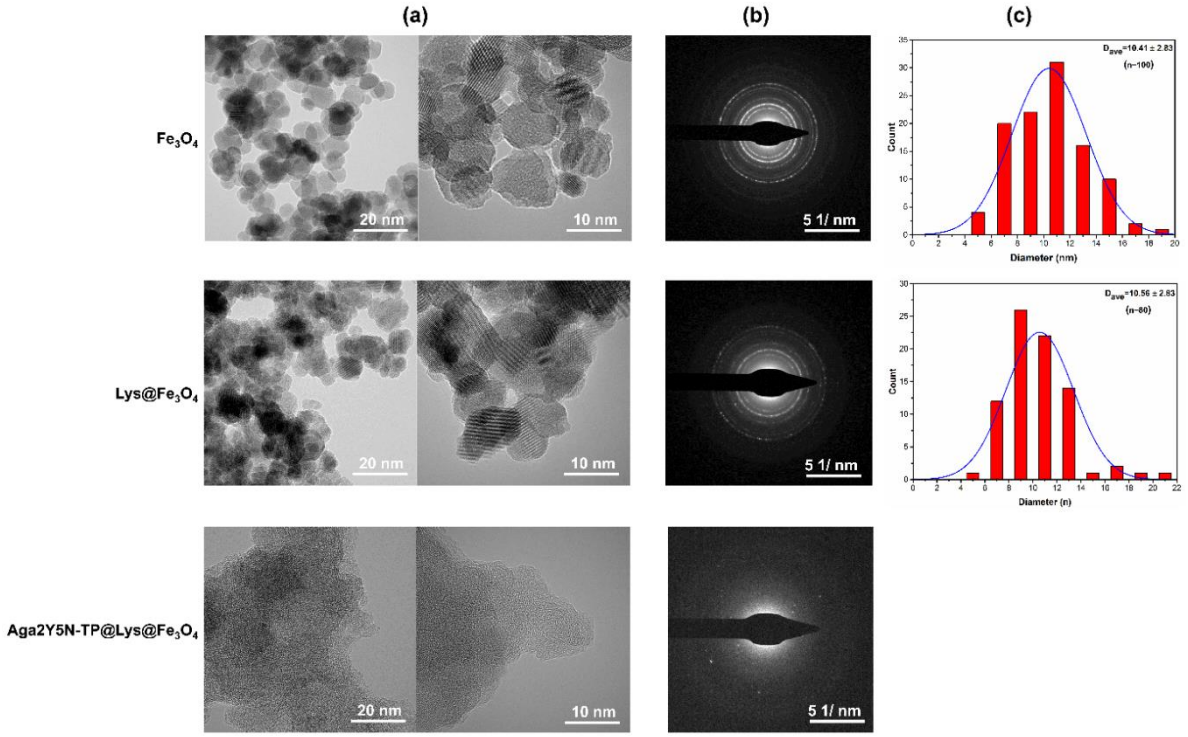


**Fig. S9** (a) TEM images, (b) SAED patterns, and (c) particles size distribution of magnetic supports and magnetic CLEA.

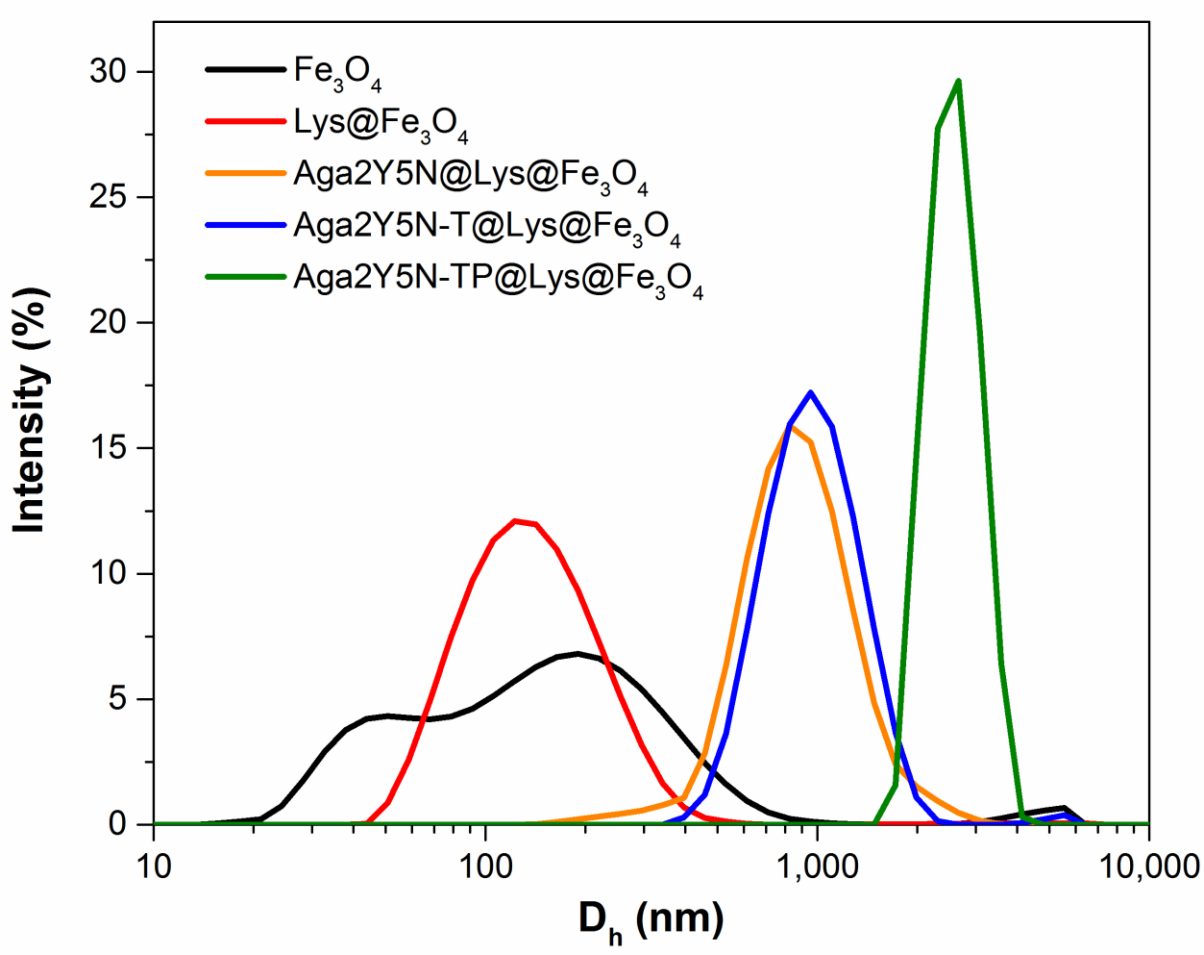


**Fig. S10** Particle size distribution of prepared magnetic supports and magnetic CLEA.

**Table S3.** Hydrodynamic diameter and polydispersity index (PDI) of magnetic particles before and after enzyme immobilization.

| Material | Hydrodynamic diameter (nm) | Polydispersity index |
|---|---|---|
| **$Fe_3O_4$** | 104.07 ± 0.43 | 0.43 ± 0.01 |
| **Lys@$Fe_3O_4$** | 106.6 3 ± 0.70 | 0.16 ± 0.02 |
| **Aga2Y5N@Lys@$Fe_3O_4$** | 775.5 ± 5.95 | 0.16 ± 0.07 |
| **Aga2Y5N-T@Lys@$Fe_3O_4$** | 894.60 ± 20.89 | 0.14 ± 0.07 |
| **Aga2Y5N-TP@Lys@$Fe_3O_4$** | 2576.33 ± 57.95 | 0.13 ± 0.18 |

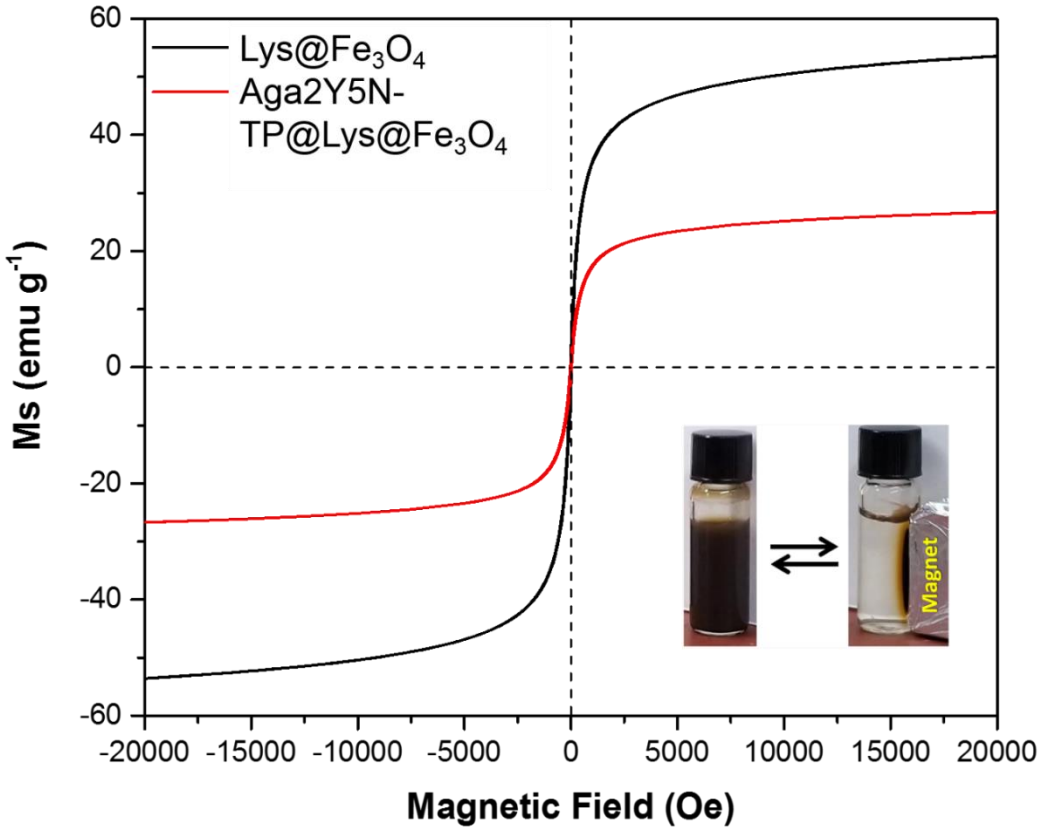


**Fig. S11** Magnetization curves of Lys@$Fe_3O_4$ and Aga2Y5N-TP@Lys@$Fe_3O_4$; inset shows separation of catalyst from the mixture by external magnet.

## Kinetics of free and magnetic CLEAs

To further observe the impact of CLEA immobilization on Aga2Y5N kinetics for agarose hydrolysis, the kinetic parameters ($V_{max}$, $K_m$, and $k_{cat}$) of free Aga2, free Aga2Y5N and Aga2Y5N-TP@Lys@$Fe_3O_4$ were determined by fitting the kinetic data to the Michaelis−Menten model (Figs. S12-S14). From the summarized kinetic parameters (Table S4), it can be seen that the $V_{max}$ of free Aga2 and free Aga2Y5N are almost similar indicating that tyrosine tagging had no detrimental effect on Aga2. Meanwhile, the $V_{max}$ of Aga2Y5N-TP@Lys@$Fe_3O_4$ was slightly reduced by 27% ($V_{max}$ = 358.6 *vs.* 260 μM $min^{-1}$). Thus, compared to free Aga2Y5N, Aga2Y5N-TP@Lys@$Fe_3O_4$ required slightly higher [S] to achieve 50% of its $V_{max}$ ($K_m$ = 3.7 g $L^{-1}$). Similarly, Aga2Y5N-TP@Lys@$Fe_3O_4$ has a lower turnover number ($k_{cat}$ = 288.7 *vs.* 209.7 $s^{-1}$) than free Aga2Y5N due to its slightly lower $V_{max}$. Reductions in $V_{max}$ and $k_{cat}$ are expected in Aga2Y5N-TP@Lys@$Fe_3O_4$ as the immobilized and cross-linked Aga2Y5N is relatively denser and rigid than its free form. Aga2Y5N-TP@Lys@$Fe_3O_4$ would also require agarose to diffuse through its CLEA layer, which also adds resistance to mass transport,[9,10] which would consequently reduce the hydrolysis rate. Nonetheless, reductions in kinetic parameters of Aga2Y5N-TP@Lys@$Fe_3O_4$ are not remarkable as sufficient amounts of hydrolysis products were still afforded within reasonable period of time. Moreover, CLEA immobilization offers numerous benefits that could compensate for this minor drawback.

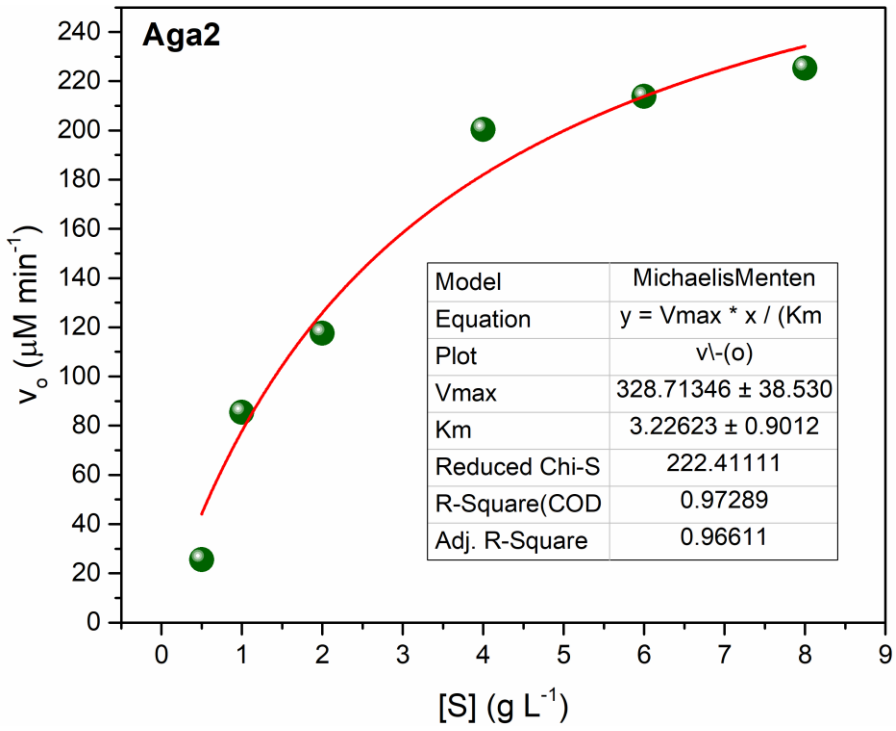


**Fig. S12** Michaelis−Menten plot of free Aga2.

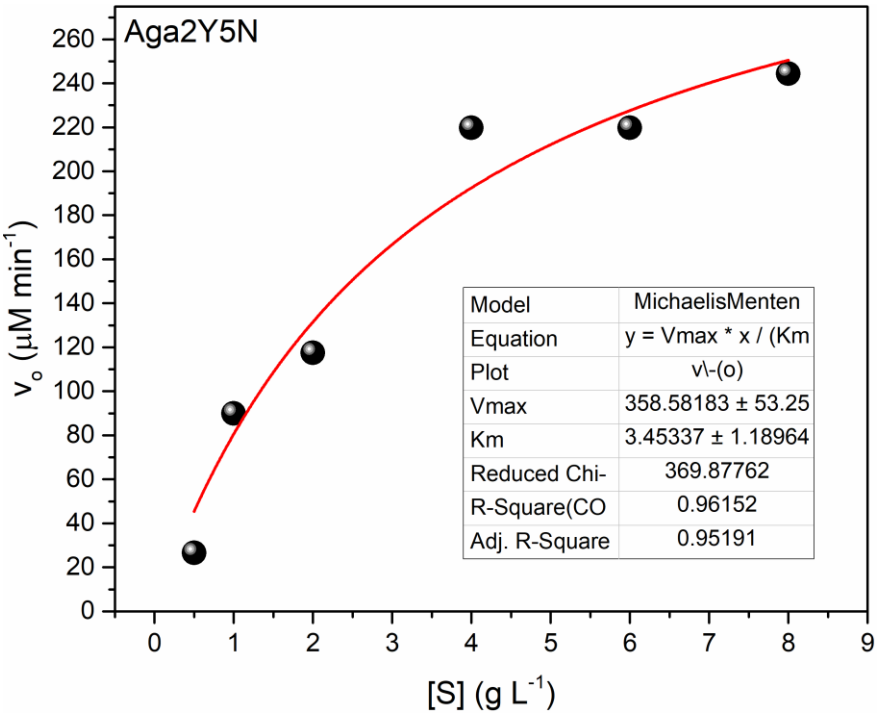


**Fig. S13** Michaelis−Menten plot of free Aga2Y5N.

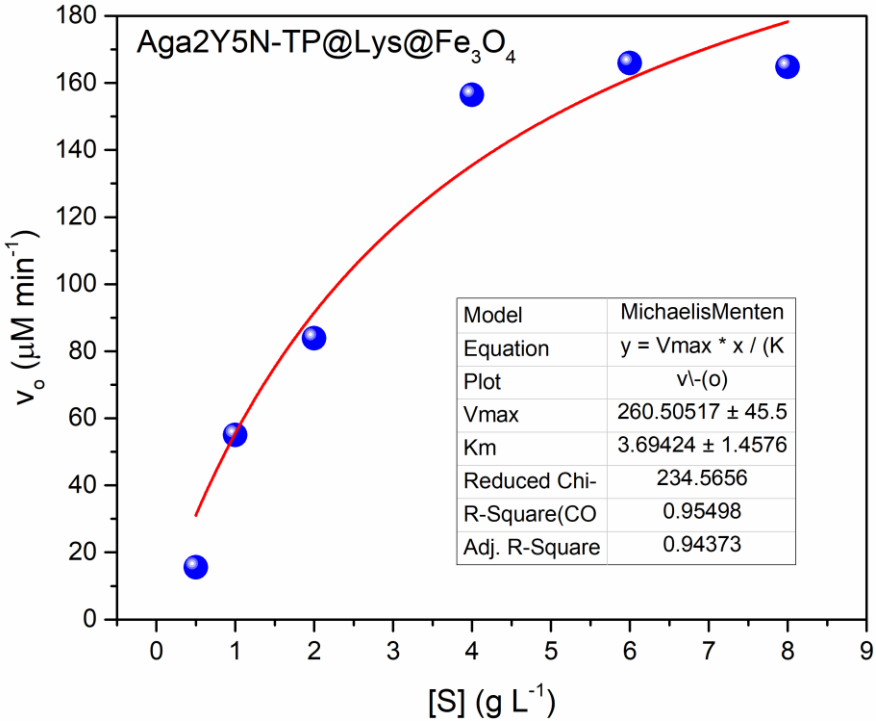


**Fig. S14** Michaelis−Menten plot of immobilized Aga2Y5N (Aga2Y5N-TP@Lys@$Fe_3O_4$).

**Table S4.** Kinetic parameters of free and immobilized β-agarase.

| Enzyme | $V_{max}$ (μM $min^{-1}$) | $K_m$ (g $L^{-1}$) | Turnover number $k_{cat}$ ($s^{-1}$) |
|---|---|---|---|
| **Aga2** | 328.7 | 3.2 | 264.7 |
| **Aga2Y5N** | 358.6 | 3.4 | 288.7 |
| **Aga2Y5N-TP@Lys@$Fe_3O_4$** | 260.5 | 3.7 | 209.7 |

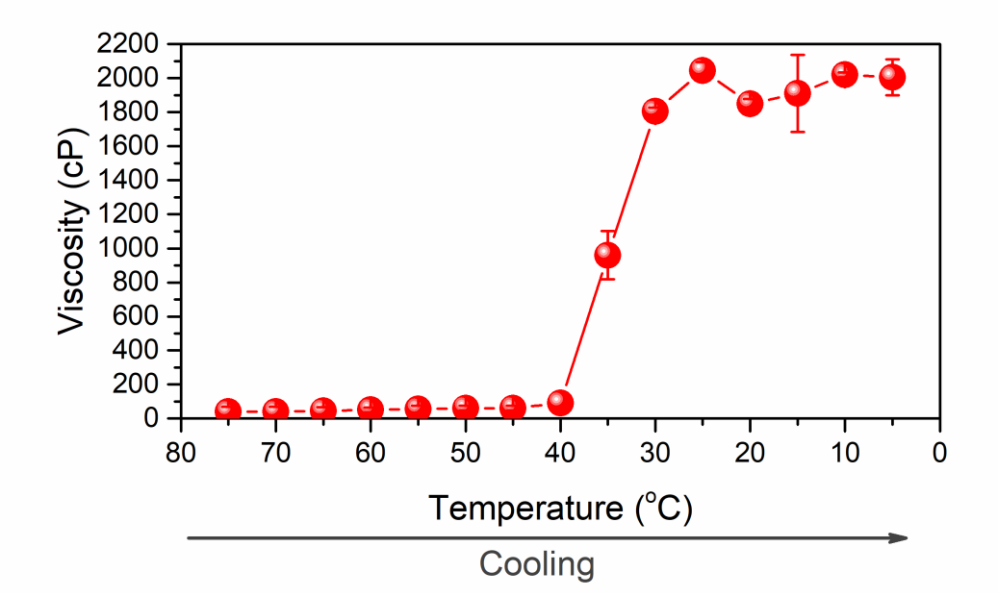


**Fig. S15** Viscosity measurements of the agar solution derived from *G. amansii* at varying temperatures from 75 ºC to 5 ºC

The sol state (i.e. low viscosity) of the agar derived from *G. amansii* was maintained until it cooled to 40 ºC. Below 40 ºC, a sharp increase in viscosity was observed due to the solidification of agar as it transitioned to its gel state. The gel became more rigid when further cooled to 5 °C. From the viscosity measurements, the sol-gel transition of the agar samples is at around ~40 ºC.

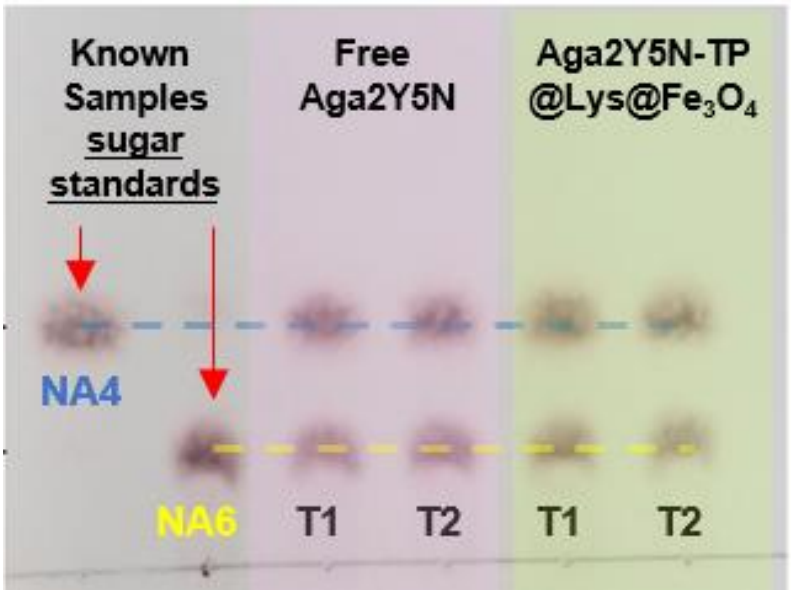


**Fig. S16** TLC analysis of products obtained after hydrolysis of agar extracted from *G. amansii* for 1 h using free and immobilized (Aga2Y5N-TP@Lys@$Fe_3O_4$) Aga2Y5N on magnetic support.

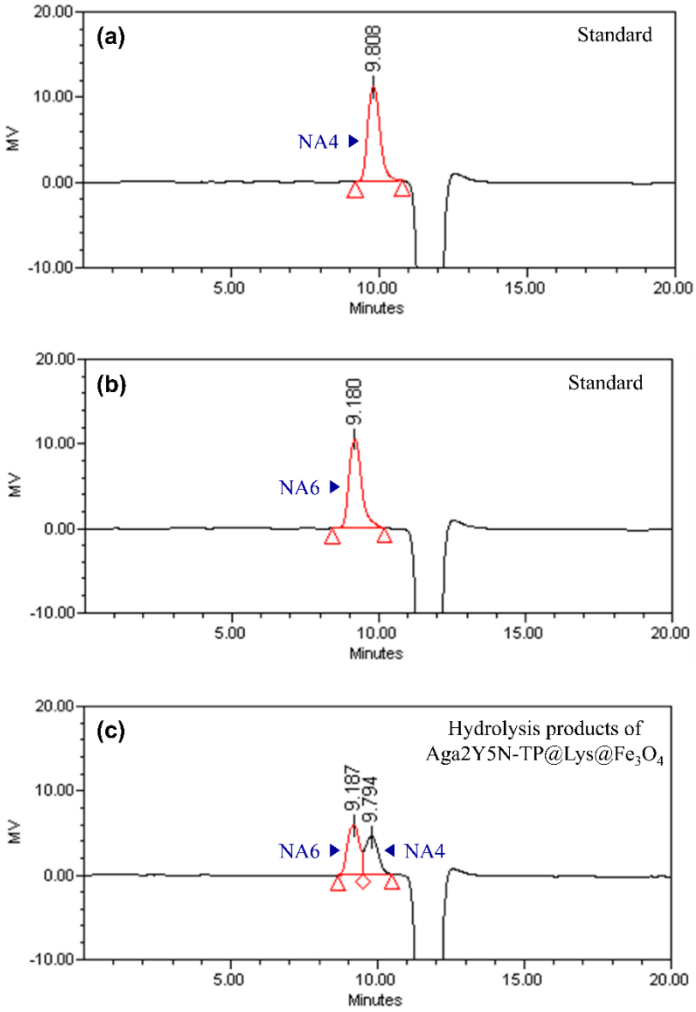


**Fig. S17** HPLC chromatograms of NAOS standards (a & b) and reaction products of Aga2Y5N-TP@Lys@$Fe_3O_4$ (c) after 48 h using agar extracted from *G. amansii* as a substrate.

In agreement with the TLC results, HPLC chromatograms of the hydrolysates from Aga2Y5N-TP@Lys@$Fe_3O_4$ detected NA4 and NA6 as products.

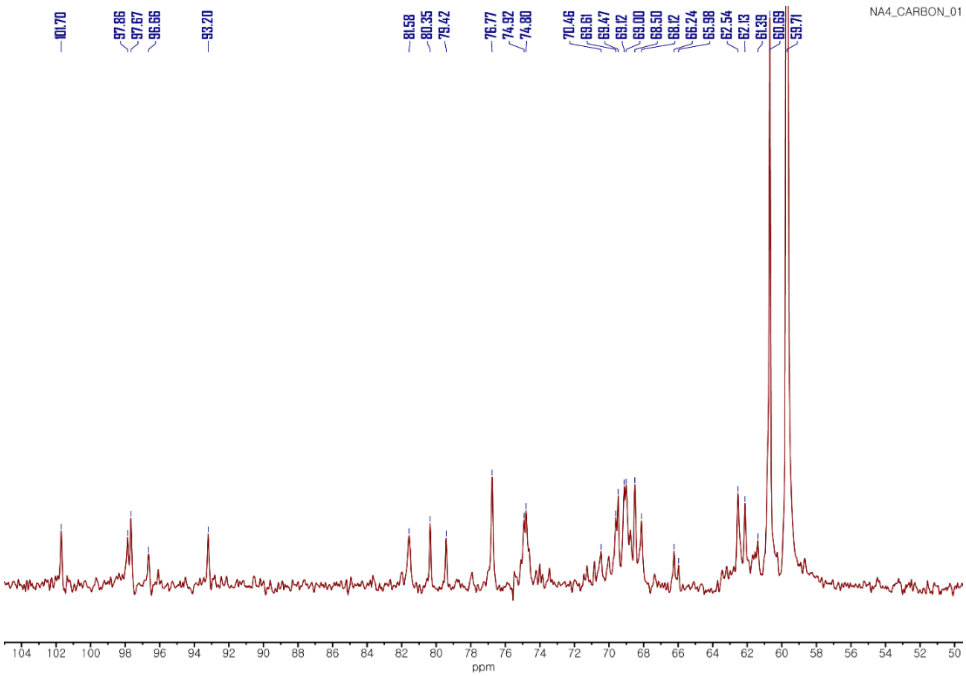


**Fig. S18** $^{13}$C NMR spectra of NA4.

The $^{13}$C NMR spectra of NA4 and NA6 are almost identical which followed the typical $^{13}$C NMR patterns reported in literature.[11,12] The spectra of both NA4 and NA6 feature resonance signals at 101.7, 97.9 and 97.7 ppm, which are typical for the C1 carbon of non-reducing D-galactose (Gnr), non-reducing 3,6-anhydo-Lgalactose (Anr) and α-anomeric form of the reducing 3,6-anhydo-Lgalactose (Arα), respectively.[11,13] Furthermore, signals at 96.7 ppm assigned to the β-anomeric (Grβ) and at 93.2 ppm for the α-anomeric (Grα) form of C1 carbon in D-galactose at the reducing end of NAOS were also identified.[11,13] The spectra also indicate the presence of multiple signals in the region 59.7-81.6 ppm, which are characteristic peaks to the other carbon atoms (C2-C6).[7] On the other hand, no signal was indicated at around 90 ppm which is typically observed when α-(1,3) linkages are hydrolyzed to form agarooligosaccharides with 3,6-anhydro-L-galactose at the reducing ends.[12-15] Thus, the $^{13}$C-NMR spectra confirm that Aga2Y5N-TP@Lys@$Fe_3O_4$ specifically hydrolyzes the β-(1,4) glycosidic linkage between D-galactose and 3,6-anhydro-L-galactose to produce NAOS with D-galactose residues at the reducing end.

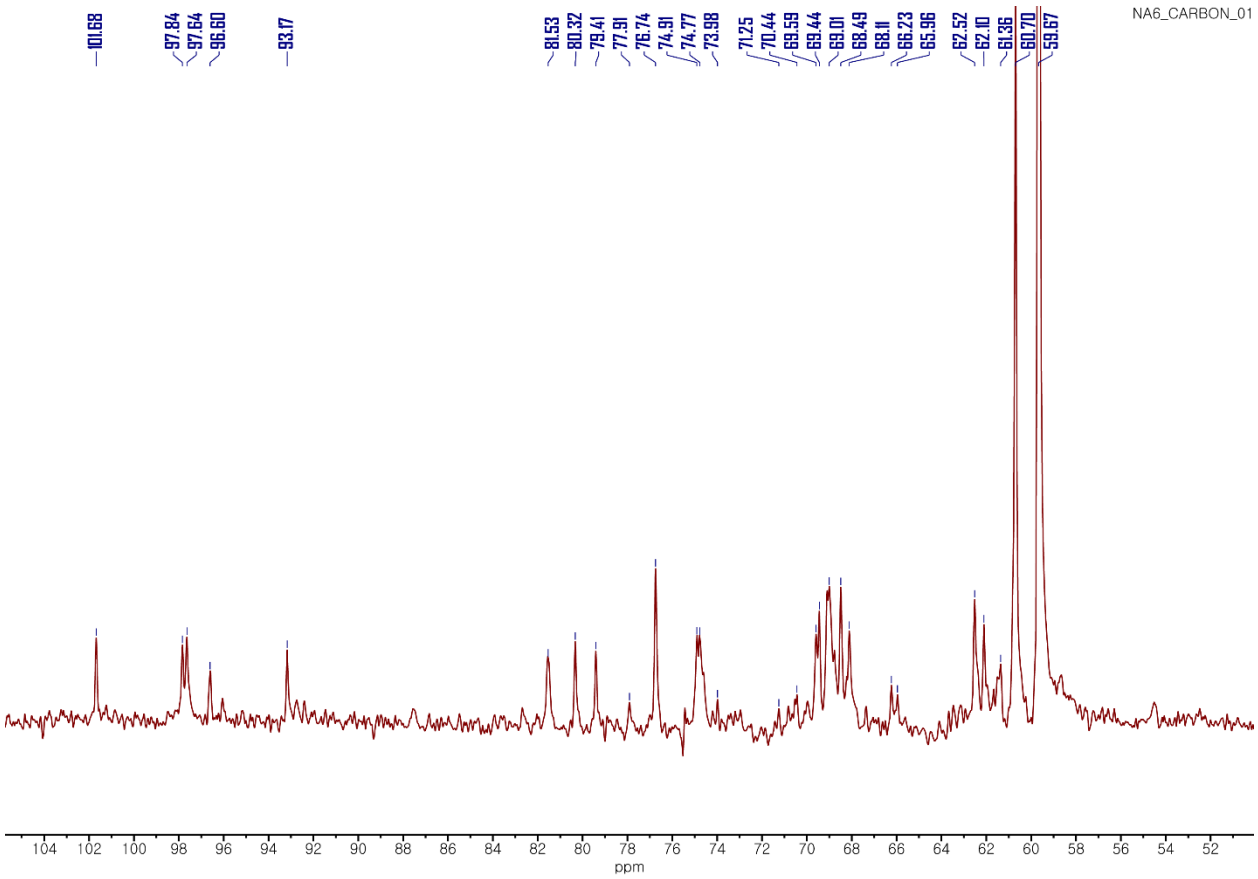


**Fig. S19** $^{13}$C NMR spectra of NA6.

**Table S5.** Aga2Y5N-TP@Lys@$Fe_3O_4$ compared with other immobilized agarases reported in literature.

| Enzyme | Support/ immobilization method | Optimum (ºC)/pH | Activity recovery (%) | Thermo-stability | Recyclability | Remarks | Ref. |
|---|---|---|---|---|---|---|---|
| | | | | Activity retention (%) (at ºC temp) | Activity retention (%) (reuse cycles) | | |
| β-agarase from *Vibrio natriegens* CICC 23820 | Tannic acid-modified MNPs/ physi-sorption | 50/6.5 | 92 | 77 (60) | 23 (7) | Enzyme leaching | 16 |
| Agarase from *Pseudomonas aeruginosa* AG LSL-11 | Amberlite IRA-900 /covalent using GA | 45/8 | 95 | 51 (60) | 49* (11) | Immobilization is non-specific | 17 |
| β-agarase *from Vibrio natriegens* CICC 23820 | Oleic Acid-Coated MNPs/covalent using GA | 40/7 | 40 | 48 (50) | 40 (7) | Immobilization is non-specific | 18 |
| β-agarase from *Marinobacter adhaerens* G4 | Polydopamine-Coated MNPs/bioadhesion | 30/7.5 | 64 | --[n.a.] | 11* (11) | Enzyme leaching | 19 |
| β-agarase from *Cellulophaga omnivescoria W5C* | Aga2Y5N-TP@Lys@$Fe_3O_4$ | 55/7 | 80 | 80 (65) | 65 (11) | Immobilization is site-specific | This study |

n.a.; Not available; * Values were extracted from plots using Web Plot Digitizer; http://arohatgi.info/WebPlotDigitizer.

**References**


(1) Zhen, Q.; Wang, M.; Qi, W.; Su, R.; He, Z. Preparation of β-Mannanase CLEAs Using Macromolecular Cross-Linkers. *Catal. Sci. Technol.* **2013**, *3* (8), 1937–1941, DOI 10.1039/c3cy20886a.

(2) Guauque Torres, M. del P.; Foresti, M. L.; Ferreira, M. L. Cross-Linked Enzyme Aggregates (CLEAs) of Selected Lipases: A Procedure for the Proper Calculation of Their Recovered Activity. AMB Express **2013**, 3, 1–11, DOI 10.1186/2191-0855-3-25.

(3) Kelley, L. A.; Mezulis, S.; Yates, C. M.; Wass, M. N.; Sternberg, M. J. E. The Phyre2 Web Portal for Protein Modeling , Prediction and Analysis. *Nat. Protoc*. **2015**, *10*, 845–858, DOI 10.1038/nprot.2015-053.

(4) Hopwood, D.; Allen, C. R.; McCabe, M. The Reactions between Glutaraldehyde and Various Proteins. An Investigation of Their Kinetics. *Histochem. J.* **1970**, *2*, 137–150, DOI 10.1007/BF01003541.

(5) Modenez, I. A.; Sastre, D. E.; Moares, F. C.; Marques Netto, C. G. C. Influence of Glutaraldehyde Cross-Linking Modes on the Recyclability of Immobilized Lipase B from Bean Oil. *Molecules*. **2018**, *23*, 1-16, DOI 10.3390/molecules23092230.

(6) Fairhead, M.; Thöny-Meyer, L. Cross-Linking and Immobilization of Different Proteins with Recombinant *Verrucomicrobium spinosum* Tyrosinase. *J. Biotechnol.* **2010**, *150*, 546–551, DOI 10.1016/j.jbiotec.2010.10.068.

(7) Isaschar-ovdat, S.; Fishman, A. Crosslinking of Food Proteins Mediated by Oxidative Enzymes – A Review. *Trends Food Sci. Technol.* **2018**, *72*, 134–143, DOI 10.1016/j.tifs.2017.12.011.

(8) Antto, R. L.; Uolanne, E. P.; Ruus, K. K.; Uchert, J. B. Tyrosinase-Aided Protein Cross-Linking: Effects on Gel Formation of Chicken Breast Myofibrils and Texture and Water-Holding of Chicken Breast Meat Homogenate Gels. *J. Agric. Food Chem.* **2007**, *55*, 1248–1255, DOI 10.1021/jf0623485.

(9) Tehrani, S. M.; Lu, Y.; Winnik, M. A. PEGMA-Based Microgels: A Thermoresponsive Support for Enzyme Reactions. *Macromolecules* **2016**, *49* (22), 8711–8721, DOI 10.1021/acs.macromol.6b01270.

(10) Hosseini, S. H.; Hosseini, S. A.; Zohreh, N.; Yaghoubi, M.; Pourjavadi, A. Covalent Immobilization of Cellulase Using Magnetic Poly(Ionic Liquid) Support: Improvement of the Enzyme Activity and Stability. *J. Agric. Food Chem.* **2018**, *66* (4), 789–798, DOI 10.1021/acs.jafc.7b03922.

(11) Lin, F.; Ye, J.; Huang, Y.; Yang, Y.; Xiao, M. Simple Preparation of Diverse Neoagaro-Oligosaccharides. *Processes* **2019**, *7*, 1–13, DOI 10.3390/pr7050267.

(12) Su, Q.; Jin, T.; Yu, Y.; Yang, M.; Mou, H.; Li, L. Extracellular Expression of a Novel β - Agarase from Microbulbifer Sp . Q7, Isolated from the Gut of Sea Cucumber. *AMB Express* **2017**, *7*, 1-9, DOI 10.1186/s13568-017-0525-8.

(13) Temuujin, U.; Chi, W.; Lee, S. Overexpression and Biochemical Characterization of DagA from Streptomyces Coelicolor A3 ( 2 ): An Endo-Type β -Agarase Producing Neoagarotetraose and Neoagarohexaose. *Appl. Microbiol. Biotechnol*. **2011**, *92*, 749–759, DOI 10.1007/s00253-011-3347-7.

(14) Wang, J.; Mou, H.; Jiang, X.; Guan, H. Characterization of a Novel β-Agarase from Marine Alteromonas Sp . SY37 – 12 and Its Degrading Products. *Appl. Microbiol. Biotechnol*. **2006**, *71*, 833–839, DOI 10.1007/s00253-005-0207-3.

(15) Chi, W. J.; Park, D. Y.; Seo, Y. B.; Chang, Y. K.; Lee, S. Y.; Hong, S. K. Cloning, Expression, and Biochemical Characterization of a Novel GH16 β -Agarase AgaG1 from Alteromonas Sp. *Appl. Microbiol. Biotechnol*. **2014**, *98*, 4545–4555, DOI 10.1007/s00253-014-5510-4.

(16) Xiao, Q.; Liu, C.; Ni, H.; Zhu, Y.; Jiang, Z.; Xiao, A. β-Agarase Immobilized on Tannic Acid-Modified Fe3O4 Nanoparticles for Efficient Preparation of Bioactive Neoagaro-Oligosaccharide. *Food Chem.* **2019**, *272*, 586–595, DOI 10.1016/j.foodchem.2018.08.017.

(17) Koti, B. A.; Shinde, M.; Lalitha, J. Repeated Batch Production of Agar-Oligosaccharides from Agarose by an Amberlite IRA-900 Immobilized Agarase System. *Biotechnol. Bioprocess Eng*. **2013**, *18*, 333–341, DOI 10.1007/s12257-012-0237-5.

(18) Xiao, A.; Xiao, Q.; Lin, Y.; Ni, H.; Zhu, Y.; Cai, H. Immobilization of Agarase from Marine Vibrio onto Carboxyl-Functioned Magnetic Nanoparticles. *J. Nanosci. Nanotechnol*. **2016**, *16*, 10048–10055, DOI 10.1166/jnn.2016.12359.

(19) Zhang, L.; Guo, X.; Song, Y.; Tang, N.; Cheng, P.; Xiang, J.; Du, W. Bioadhesive Immobilize Agarase on Magnetic Ferriferous by Polydopamine. *Mater. Sci. Eng. C* **2018**, *93*, 218–225, DOI 10.1016/j.msec.2018.07.068.